Downlink resource allocation for dynamic TDMA-based VLC systems

Amr M. Abdelhady, Osama Amin, Anas Chaaban, Basem Shihada and Mohamed-Slim Alouini

Abstract

Visible light communications (VLC) in general and resource allocation for VLC networks particularly have gained lots of attention recently. In this work, we consider the resource allocation problem of a VLC downlink transmission system employing dynamic time division multiple access where time and power variables are tuned to maximize spectral efficiency (SE). As for the operational conditions, we impose constraints on the average optical intensity, the energy budget and the quality-of-service. To solve the non-convex problem, we transform the objective function into a difference of concave functions by solving a second order differential inequality. Then, we propose a low-complexity algorithm to solve the resource allocation problem. Finally, we show by simulations the SE performance gains achieved by optimizing time and power allocation over the initial total power minimization solution for the considered system.

I. Introduction

Optical wireless communications (OWC) has gained lots of interest to mitigate the spectrum scarcity and the ever-exploding demand on wireless data traffic [2]. OWC offers alternative transmission options through infrared, visible light, and ultraviolet bands. The superiority of OWC systems over their radio frequency counterparts appears clearly in terms of area spectral efficiency (SE), which in turn gives it the advantage to be one of the key promising technologies

A. M. Abdelhady, O. Amin, B. Shihada and M.-S. Alouini are with with the Computer Electrical, and Mathematical Science and Engineering (CEMSE) Division, King Abdullah University of Science and Technology (KAUST), Thuwal, Makkah Province, Kingdom of Saudi Arabia, E-mail: {amr.abdelhady, osama.amin, basem.shihada, slim.alouini}@kaust.edu.sa.

A. Chaaban is with the School of Engineering, Okanagan Campus, University of British Columbia, Canada, E-mail: anas.chaaban@ubc.ca.

A part of this paper that investigates a simpler version of the considered problem is published in [1].

for 5G networks [3]. Furthermore, the energy consumption of optical transmitters such as light emitting diodes (LEDs) is lower than its counterpart in RF spectrum [4]. Among the optical frequency bands, the visible light band is of special interest for different reasons. The visible light infrastructure built for illumination purposes can be used in communications, thanks to the development of LED devices for lighting. LED can be switched at very high rates supporting fast data transmission and providing in the same time higher illumination efficacies than traditional lamps. Moreover, visible light is safer to human health than infrared and ultraviolet waves, which alleviates transmitted power restriction limits for visible light communications (VLC). Furthermore, VLC systems are more energy efficient, because the paid energy cost covers two simultaneous services, i.e., lighting and communications.

The advantages offered by VLC systems in supporting multiple services are associated with some challenges [5]. The VLC system designers should take illumination constraints into consideration [6]. In addition, it is desirable to avoid flickering, maintain chromaticity of the VLC transmitter and support dimming and color control capabilities. As for the communication service, it suffers from the relatively small spatial coverage of the LED source, which requires deployment of a large number of LEDs and controlling frequent handovers that will occur consequently. VLC links are highly sensitive to the availability of line-of-sight (LOS), i.e. high data rates are achievable only if LOS exists. Moreover, uplink implementation in VLC is a major issue as it is inconvenient to install an illuminating LED at the mobile terminal, so infrared or modulating retro-reflectors can be used instead.

To optimize VLC systems performance, the system available resources should be allocated properly to users while taking indoor lighting constraints into consideration. Resource allocation problems with various objectives for VLC networks have been investigated in different contexts [7]–[16]. In [8], Chaaban *et al.* considered the power allocation problem to maximize the achievable rate for optical wireless parallel channels with total light intensity constraint. In [9], Gong *et al.* considered rate maximization and total power minimization problems by optimizing power allocation of each color LED subject to minimum and maximum illumination constraints, and constant chromaticity. In [10] Jiang *et al.* studied power allocation for a multi-user downlink VLC system subject to chromaticity, illumination, and amplitude constraints with the objective of maximizing the sum-rate of the setup. In [12] Shen *et al.* optimized transmit beamforming to maximize the achievable sum rate of the downlink of a VLC system subject to transmit power constraints. In [13], Shen *et al.* considered the downlink of a Multi Input Single Output (MISO)

VLC system where zero-forcing beamforming vector is optimized to maximize the sum rate of the setup. In [14] Bykhovsky *et al.* considered power allocation, user association, and subcarrier allocation to maximize the minimum user rate of a multi-cell VLC system subject to a total power constraint. Note that a practical system generally combines a multitude of constraints (optical intensity, electrical energy consumption, and quality of service (QoS)).

In this paper, we consider the downlink of a VLC cell that serves a number of users through time division multiple access (TDMA). In fact, TDMA is of special interest due to its relatively high power efficiency [17], and its integrability with other multiple access schemes as code division multiple access (CDMA) and space division multiple access (SDMA) [18], [19]. Dynamic TDMA system can adds additional degree of freedom in illumination control through the adaptive time allocation. On the other hand, CDMA has the highest electrical power requirements due to the increasing effect of inter-symbol-interference [20]. Moreover, orthogonal frequency division multiple access (OFDMA) suffers from high peak-to-average power ratio problem [21]. We investigate joint time and power allocation problem that maximizes the SE of this system considering a set of constraints on the energy consumption, light intensity and QoS. In contrast to its RF counterpart with the celebrated water-filling solution, this problem is much harder because of the inherent non-convexity of its objective function. Due to this non convexity, to solve the maximization problem, we transform it to a difference of convex/concave (DC) programming formulation. This reformulation is achieved by introducing an auxiliary function that is found by solving a differential equation. We propose a low-complexity algorithm to solve the problem iteratively by solving a series of convex optimization problems. To the best of our knowledge, the joint time and power resource allocation problem along with the considered constraints has not been considered before in the literature.

The rest of this paper is organized as follows, in section II we present the adopted system model of this work, then in section III we provide the mathematical formulation of the considered SE maximization problem and explain our proposed algorithm to solve it. After that, in section IV we test the proposed algorithm by extensive simulations for different parameter values and compare its performance against two algorithms with varying complexity. Finally we present the paper conclusion in section V.

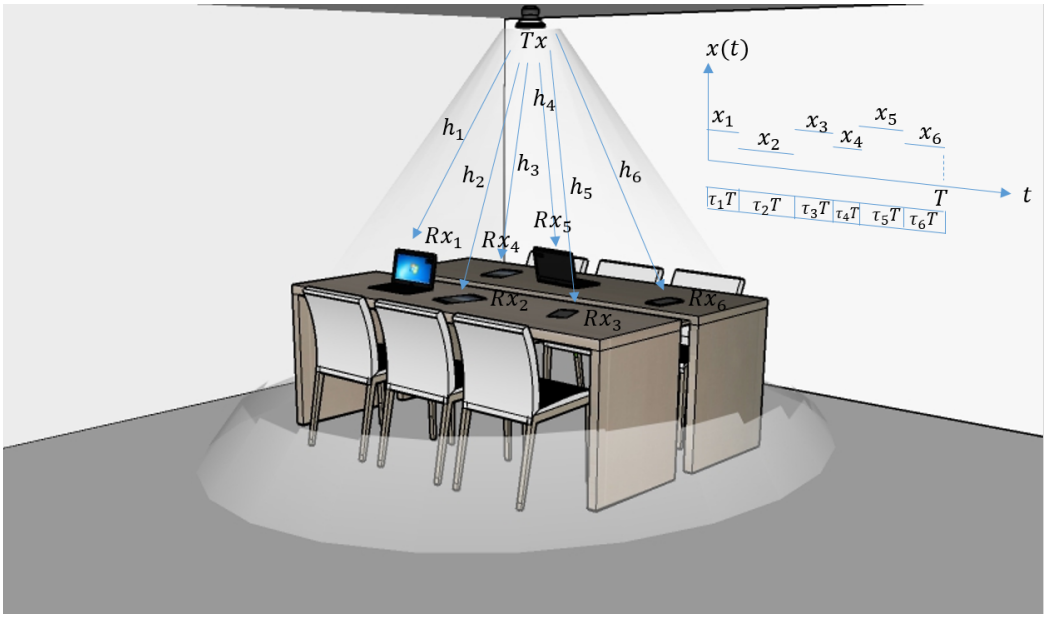

Fig. 1: Single VLC cell model with dynamic TDMA concept.

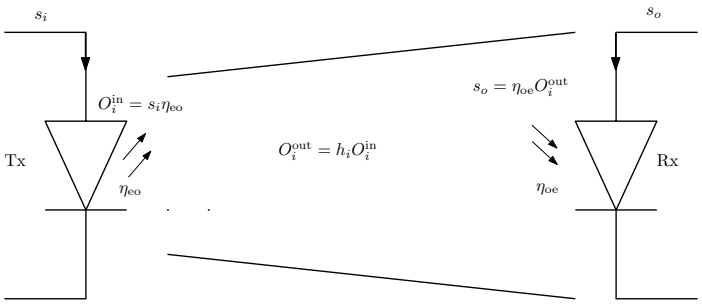

Fig. 2: VLC Link Model

II. System and Channel Model

Consider the downlink of a single cell VLC system where a single LED transmitter is used to serve K users via dynamic TDMA, where the transmitter communicates with each user at a different time-slot, i.e. each user experiences an interference free channel, with varying durations as could be seen in Fig. 1. In this setup, the transmitter encodes different users' data streams using the LED excitation current at each user's time-slot, and controls the durations of time-slots allocated to each user and the average LED excitation current during each time-slot within the transmission frame aiming at maximizing a certain network utility function such as the overall SE whilst satisfying the imposed average illumination constraint, transmission rate requirements

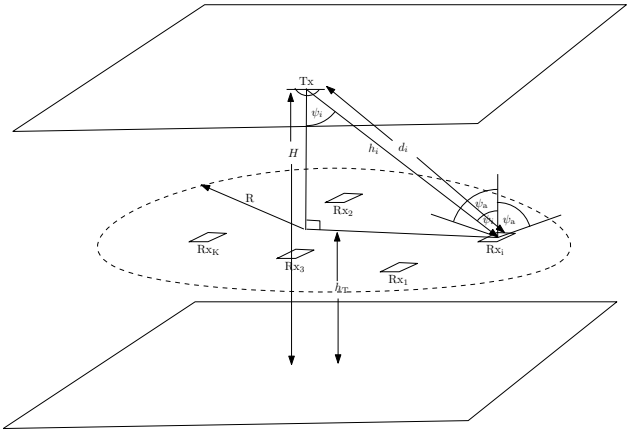

Fig. 3: Channel Model

for all users, minimum time slot duration imposed by the LED modulation bandwidth, and total energy consumption per transmission frame.

At its corresponding time slot, each receiver converts the received optical signal to an electrical one and then the detection process is performed to extract the transmitted symbols as shown in Fig. 2.The received signal at the i-th user can be modeled as

$$y_i = h_i \eta_{\text{eo}} \eta_{\text{oe}} s_i + n_i, \tag{1}$$

where s_i is the current intensity used to transmit a symbol to the i-th user, η_{eo} is the efficiency of converting the electrical signal s_i to the transmitted optical signal O_i^{in}, η_{oe} is the efficiency of converting the received optical signal O_i^{out} to electrical signal s_o, and h_i is the VLC channel gain coefficient between the transmitter and the i-th receiver, and n_i is a zero mean additive white Gaussian noise with variance σ_n^2. The transmission frame period T is divided between the users such that the VLC and the time slot duration of each user is $\tau_i T$, where $\sum_{i=1}^{K} \tau_i = 1$. The average energy consumed for each transmitted frame is $T \sum_{i=1}^{K} \tau_i \mathbb{E}\{s_i^2\} \leq E_{\text{v}}$, where E_{v} is the transmitter energy constraint. The average optical intensity per time slot is $\sum_{i=1}^{K} \tau_i \mathbb{E}\{s_i\} \eta_{\text{eo}} = I_{\text{eo}}$, where I_{eo} is the average optical intensity constraint (lighting constraint).

As for the channel model presented in Fig. 3, we adopt the followed channel model in [22] where the channel gain h_i between the transmitter and receiver i depends solely on the relative position of the receiver with respect to the transmitter, and is given by:

$$h_i = \frac{(m+1) A_{\text{PD}}}{2\pi d_i^2} \cos^{m+1}(\psi_i) \text{rect}\left(\frac{\psi_i}{\psi_{\text{a}}}\right), \tag{2}$$

where $m = -\ln 2/\ln(\cos(\phi_{\rm a}))$ is the Lambertian order, $\phi_{\rm a}$ is the semi-angle at half-power of the light source emission pattern, $R_{\rm PD}$ is the photo-detector responsivity $A_{\rm PD}$ is the effective photo-detector area, d_i is the distance between the transmitter and user i, ψ_i is the angle between the incident light ray and the normal to the photo-detector plane, $\psi_{\rm a}$ is the field of view of the user's receiver, and rect(x) is the rectangular function defined as rect$(x) = 1$ if $|x| \leq 1$, and 0 otherwise. We assume perfect knowledge of h_i $\forall i$ at the transmitter. In the quasi-static channel model, h_i maintains the same value throughout a transmission block, and changes in between blocks due to change of location.

III. Spectral Efficiency Optimization

In this section, we study the resource allocation problem of the downlink of a VLC system to maximize its SE. To this end, we express the overall system SE using the achievable SE of optical IM/DD channels lower bound presented in [23, eq. 26], with s_i being drawn randomly from an exponential distribution with rate parameter $1/x_i$, i.e., $s_i \sim \exp(1/x_i)$, as

$$\eta_{\rm SE} = \frac{1}{2}\sum_{i=1}^{K} \tau_i \log_2\left(1+\gamma_i x_i^2\right), \tag{3}$$

where, γ_i is the i-th user VLC channel-to-noise ratio defined as $\gamma_i = \frac{e}{2\pi}\eta_{\rm eo}^2\eta_{\rm oe}^2/\sigma_n^2 h_i^2$, $x_i = \mathbb{E}\{s_i\}$. The resource allocation problem aims to compute the average current intensity vector $\mathbf{x} = \{x_i\}_{i=1}^K$ and time fraction allocation vector $\boldsymbol{\tau} = \{\tau_i\}_{i=1}^K$ according to the following optimization problem:

$$\begin{aligned}
\textbf{(P1)} \quad \max_{\mathbf{x},\boldsymbol{\tau}} \quad & \eta_{\rm SE} \\
\text{subject to} \quad & {\rm C1}: \sum_{i=1}^{K} \tau_i x_i^2 \leq P_{\rm M} \\
& {\rm C2}: \sum_{i=1}^{K} \tau_i x_i = I \\
& {\rm C3}: R_i(x_i,\tau_i) \geq R_{\rm th} \quad \forall i \\
& {\rm C4}: \sum_{i=1}^{K} \tau_i = 1 \\
& {\rm C5}: \tau_i \geq \tau_\epsilon, x_i \geq 0 \quad \forall i,
\end{aligned}$$

where $P_{\mathrm{M}} = \frac{E_{\mathrm{v}}}{2T}$, $I = \frac{I_{\mathrm{eo}}}{\eta_{\mathrm{eo}}}$, and $R_i\left(x_i, \tau_i\right) = \frac{1}{2} B_{\mathrm{v}} \tau_i \log_2\left(1 + \gamma_i x_i^2\right) \quad \forall i$. As for the constraints: $\mathrm{C1}$ guarantees that the total energy consumption of the transmitter does not exceed the available budget. $\mathrm{C2}$ guarantees fixed average optical intensity by fixing the average current intensity used at the transmitter and $\mathrm{C3}$ guarantees a minimum rate of R_{th} for each user, which can be selected based on the applications or services that is going to be supported by the network and expected number of users to be served. As for $\mathrm{C4}$, it is adopted to ensure that the total allocated time durations consume the transmission frame while $\mathrm{C5}$ enforces that each user is allocated a minimum amount of time due to practical switching limitations and secures the non-negativity of the average LED current being allocated during each time slot.

It can be shown that $\mathbf{(P1)}$ is a non-convex problem. To solve this problem, we first adopt the transformation of variables ($z_i = \tau_i x_i$), which reformulates $\mathbf{(P1)}$ to:

$$
\begin{aligned}
\mathbf{(\tilde{P}1)} \quad \max_{\mathbf{z},\boldsymbol{\tau}} \quad & \frac{1}{2} \sum_{i=1}^{K} \tau_i \ln\left(1 + \gamma_i \frac{z_i^2}{\tau_i^2}\right) \\
\text{subject to} \quad & \mathrm{C1}' : \sum_{i=1}^{K} \frac{z_i^2}{\tau_i} \leq P_{\mathrm{M}} \\
& \mathrm{C2}' : \sum_{i=1}^{K} z_i = I \\
& \mathrm{C3}' : R_i\left(z_i, \tau_i\right) \geq R_{\mathrm{th}} \quad \forall i \\
& \mathrm{C4}, \mathrm{C5}.
\end{aligned}
$$

Unlike $\mathbf{P1}$, $\mathbf{\tilde{P}1}$ can be written in a DC format allowing us to solve it in a tractable way. In the following subsections, we first explain how $\mathbf{(\tilde{P}1)}$ can be transformed into a DC optimization problem. Then, we employ successive convex approximation (SCA) to find a solution of the DC problem by solving alternatively two convex problems: power and time allocation. Finally, we summarize the proposed approach that jointly allocate the find a joint power and time allocation solution.

A. DC programming problem reformulation and proposed solution

The objective function of $\mathbf{(\tilde{P}1)}$ is not concave in the considered optimization variables. This objective function is a sum of functions having the form $\tau \ln\left(1 + \gamma \frac{z^2}{\tau^2}\right)$[1], which we reformulate into a difference of two concave functions based on the following proposition:

[1]Here, the variable z is used to represent z_i for any arbitrary index i, the index is dropped for convenience.

Proposition 1. *The non-convex function* $f(\tau, z; \gamma) = \tau \ln\left(1 + \gamma \frac{z^2}{\tau^2}\right)\ \forall \tau > 0$ *can be expressed as a difference of two concave functions as:*

$$f(\tau, z; \gamma) = -\frac{\rho z^2}{2\tau} - \tau \ln\left(\frac{1 + \gamma \frac{z^2}{\tau^2}}{e^{-\frac{\rho z^2}{2\tau^2}}}\right), \tag{4}$$

where $\rho = \frac{\gamma}{4}$.

Proof. The proof is given in Appendix A. □

The objective function of $(\tilde{\mathbf{P}}\mathbf{1})$ encompasses K versions of the function $f(\tau, z; \gamma)$. Thus, we need K different ρ to use Proposition 1 directly to do the DC reformulation. Alternatively, we use a unified $\hat{\rho}$ that guarantees the validity of the DC decomposition for all values of i with $\hat{\rho} = \max_i \rho_i$, where $\rho_i = \frac{\gamma_i}{4}$.

Now, we apply the result of Proposition 1 on $(\tilde{\mathbf{P}}\mathbf{1})$ in order to express it in a DC programming problem as

$$\begin{aligned} (\mathbf{P2}) \quad \max_{\mathbf{z},\boldsymbol{\tau}} \quad & -\sum_{i=1}^{K} \left(\frac{\hat{\rho} z_i^2}{2\tau_i} + \tau_i \ln\left(\frac{e^{-\frac{z_i^2}{\tau_i^2}\hat{\rho}/2}}{1 + \frac{\gamma_i z_i^2}{\tau_i^2}} \right) \right), \\ \text{subject to} \quad & \mathrm{C1}' - \mathrm{C3}', \mathrm{C4}, \mathrm{C5}. \end{aligned}$$

To solve $(\mathbf{P2})$, we use SCA procedure to approximate the objective function using its first order Taylor series approximation and solve the following convex optimization problem successively

$$\begin{aligned} (\mathbf{P3}) \quad \max_{\mathbf{z},\boldsymbol{\tau}} \quad & -\sum_{i=1}^{K} \left(\frac{\hat{\rho} z_i^2}{2\tau_i} + \tilde{g}_i\left(z_i, \tau_i, \bar{z}_i, \bar{\tau}_i\right) \right) \\ \text{subject to} \quad & \mathrm{C1}', \mathrm{C2}', \mathrm{C4}, \mathrm{C5}, \\ & \mathrm{C6}: \tilde{R}_i \geq \ln(2) R_{\mathrm{th}} \quad \forall i \end{aligned}$$

where $\tilde{R}_i = -\frac{\hat{\rho}}{2} B_{\mathrm{v}} \frac{z_i^2}{\tau_i} - B_{\mathrm{v}} \tilde{g}_i\left(z_i, \tau_i, \bar{z}_i, \bar{\tau}_i\right)$, $\tilde{g}_i\left(z_i, \tau_i, \bar{z}_i, \bar{\tau}_i\right)$ is the first order Taylor series approximation of the second term in the objective function of $(\mathbf{P2})$ around $\bar{z}_i, \bar{\tau}_i$, which is expressed as

$$\tilde{g}_i\left(z_i, \tau_i, \bar{z}_i, \bar{\tau}_i\right) = \bar{\tau}_i \ln\left(\frac{e^{-\frac{\bar{z}_i^2}{\bar{\tau}_i^2}\hat{\rho}/2}}{1 + \gamma_i \frac{\bar{z}_i^2}{\bar{\tau}_i^2}} \right) - a_i\left(z_i - \bar{z}_i\right) + b_i\left(\tau_i - \bar{\tau}_i\right), \tag{5}$$

where a_i is defined as

$$a_i = \frac{2\bar{z}_i \bar{\tau}_i \gamma_i}{\bar{\tau}_i^2 + \bar{z}_i^2 \gamma_i} + \frac{\hat{\rho} \bar{z}_i}{\bar{\tau}_i}, \tag{6}$$

and b_i is defined as

$$b_i = \frac{2\bar{z}_i^2\gamma_i}{\bar{\tau}_i^2 + \bar{z}_i^2\gamma_i} + \frac{\hat{\rho}\bar{z}_i^2}{\bar{\tau}_i^2} + \ln\left(\frac{e^{-\frac{\bar{z}_i^2}{\bar{\tau}_i^2}\hat{\rho}/2}}{1+\gamma_i\frac{\bar{z}_i^2}{\bar{\tau}_i^2}}\right). \tag{7}$$

Now, we solve $\mathbf{(P3)}$ by dividing the optimization variables into two vectors $\boldsymbol{\tau}$ and $\boldsymbol{z}$ where we keep one of them constant while optimizing the other and then switch between them until convergence. Therefore, the solution of $\mathbf{(P3)}$ is obtained by solving two subproblems, one to optimize the fractional time, i.e., $\boldsymbol{\tau}$, while the other one optimizes the weighted current intensity, i.e. $\boldsymbol{z}$, as will be analyzed in the following subsections.

B. Weighted current intensity allocation

Define the $\boldsymbol{z}$ optimization problem for a fixed $\boldsymbol{\tau}$ as

$$\begin{aligned}\mathbf{(P3\,a)} \quad \max_{\mathbf{z}} \quad & -\sum_{i=1}^{K}\left(\frac{\hat{\rho}z_i^2}{2\tau_i} + \tilde{g}_i\left(z_i,\tau_i,\bar{z}_i,\bar{\tau}_i\right)\right)\\ \text{subject to} \quad & \mathrm{C1}', \mathrm{C2}', \mathrm{C6},\\ & \mathrm{C5a}\ z_i \geq 0\ \forall i.\end{aligned}$$

We can further simplify $\mathbf{(P3\,a)}$ by reducing C5a and C6 to be C7a: $(z_{\min,i} \leq z_i \leq z_{\max,i} \quad \forall i)$ as shown below:

$$\mathrm{C6}: \left(-\frac{\hat{\rho}B_{\mathrm{v}}z_i^2}{2\tau_i} - B_{\mathrm{v}}\left(\bar{\tau}_i\ln\left(\frac{e^{-\frac{\hat{\rho}\bar{z}_i^2}{2\bar{\tau}_i^2}}}{1+\gamma_i\frac{\bar{z}_i^2}{\bar{\tau}_i^2}}\right) - a_i\left(z_i-\bar{z}_i\right) + b_i\left(\tau_i-\bar{\tau}_i\right)\right)\right) \geq \ln(2)R_{\mathrm{th}} \tag{8}$$

By defining ζ_i as:

$$\zeta_i = -B_{\mathrm{v}}\bar{\tau}_i\ln\left(\frac{e^{-\frac{\hat{\rho}\bar{z}_i^2}{2\bar{\tau}_i^2}}}{1+\frac{\gamma_i\bar{z}_i^2}{\bar{\tau}_i^2}}\right) - B_{\mathrm{v}}a_i\bar{z}_i - B_{\mathrm{v}}b_i\left(\tau_i-\bar{\tau}_i\right) - \ln(2)R_{\mathrm{th}} \tag{9}$$

The bounds of C7a can be calculated as:

$$z_{\min,i} = \max\left(0, \left(B_{\mathrm{v}}a_i - \sqrt{B_{\mathrm{v}}^2a_i^2 + 2B_{\mathrm{v}}\frac{\hat{\rho}}{\tau_i}\zeta_i}\right)\frac{\tau_i}{B_{\mathrm{v}}\hat{\rho}}\right) \tag{10}$$

$$z_{\max,i} = \left(B_{\mathrm{v}}a_i + \sqrt{B_{\mathrm{v}}^2a_i^2 + 2B_{\mathrm{v}}\frac{\hat{\rho}}{\tau_i}\zeta_i}\right)\frac{\tau_i}{B_{\mathrm{v}}\hat{\rho}} \tag{11}$$

The Lagrangian of $\mathbf{P3a}$ can be formulated as:

$$\mathcal{L}_{\mathrm{a}} = -\frac{\hat{\rho}}{2}\sum_{i=1}^{K}\frac{z_i^2}{\tau_i} - \sum_{i=1}^{K}\tilde{g}_i\left(z_i,\tau_i,\bar{z}_i,\bar{\tau}_i\right) + \mu_{\mathrm{a}}\left(P_{\mathrm{M}} - \sum_{i=1}^{K}\frac{z_i^2}{\tau_i}\right) + \lambda_{\mathrm{a}}\left(I - \sum_{i=1}^{K} z_i\right) + \sum_{i=1}^{K}\nu_{\mathrm{a},i}\left(z_{\max,i} - z_i\right) + \sum_{i=1}^{K}\alpha_{\mathrm{a},i}\left(z_i - z_{\min,i}\right) \tag{12}$$

By applying the Karush-Kuhn-Tucker (KKT) conditions, we get

$$\frac{\partial\mathcal{L}_{\mathrm{a}}}{\partial z_i} = -\hat{\rho}\frac{z_i}{\tau_i} + a_i - 2\mu_{\mathrm{a}}\frac{z_i}{\tau_i} - \lambda_{\mathrm{a}} - \nu_{\mathrm{a},i} + \alpha_{\mathrm{a},i} = 0 \quad \forall i \tag{13}$$

$$\mu_{\mathrm{a}}\left(P_{\mathrm{M}} - \sum_{i=1}^{K}\frac{z_i^2}{\tau_i}\right) = 0 \tag{14}$$

$$\nu_{\mathrm{a},i}\left(z_{\max,i} - z_i\right) = 0\ \forall i, \alpha_{\mathrm{a},i}\left(z_i - z_{\min,i}\right)\ \forall i \tag{15}$$

$$\mu_{\mathrm{a}} \geq 0, \nu_{\mathrm{a},i} \geq 0\ \forall i, \alpha_{\mathrm{a},i} \geq 0\ \forall i \tag{16}$$

The convexity of $\mathbf{(P3\,a)}$ implies that strict complementary slackness applies. From the power budget constraint C1 perspective, we have two possibilities

- (i) $\mu_{\mathrm{a}} = 0, \sum_{i=1}^{K}\frac{z_i^2}{\tau_i} < P_{\mathrm{M}}$
- (ii) $\mu_{\mathrm{a}} > 0, \sum_{i=1}^{K}\frac{z_i^2}{\tau_i} = P_{\mathrm{M}}$.

For scenario (i), the optimal values of $\mathbf{z}$ elements are calculated as follows in terms of (λ_{a} and μ_{a}):

$$z_i^* = \begin{cases} z_{\min,i} & \forall i \in U_{\min} \\ \tau_i\frac{a_i - \lambda_{\mathrm{a}}}{\hat{\rho}+2\mu_{\mathrm{a}}} & \forall i \in \bar{U} \\ z_{\max,i} & \forall i \in U_{\max}, \end{cases} \tag{17}$$

where $\bar{U} = \{i : z_{\min,i} < z_i^* < z_{\max,i}\}$, $U_{\min} = \{i : z_i^* = z_{\min,i}\}$, $U_{\max} = \{i : z_i^* = z_{\max,i}\}$ with $\bar{U} \cup U_{\min} \cup U_{\max} = \{1,\ldots,K\}$, such that $\bar{U}, U_{\min},$ and $U_{\max}$ are mutually exclusive. We substitute (17) in C2 and solve for λ_{a} getting

$$\lambda_{\mathrm{a}} = \left(\left(I - \sum_{i\in U_{\min}} z_{\min,i} - \sum_{i\in U_{\max}} z_{\max,i}\right)(\hat{\rho}+2\mu_{\mathrm{a}}) - \sum_{i\in\bar{U}}\tau_i a_i\right) / \left(-\sum_{i\in\bar{U}}\tau_i\right) \tag{18}$$

By defining d, f, and $\mathcal{X}$ as follows:

$$d = \left(I - \sum_{i \in U_{\min}} z_{\min,i} - \sum_{i \in U_{\max}} z_{\max,i} \right) / \left(- \sum_{i \in \bar{U}} \tau_i \right), \tag{19}$$

$$f = \sum_{i \in \bar{U}} \tau_i a_i / \sum_{i \in \bar{U}} \tau_i, \tag{20}$$

$$\mathcal{X} = \hat{\rho} + 2\mu_{\mathrm{a}}. \tag{21}$$

We can then express λ_{a} as:

$$\lambda_{\mathrm{a}} = d\mathcal{X} + f \tag{22}$$

By substituting (22) in $\mathbf{C1}$ and solving for μ_{a} we get:

$$\mu_{\mathrm{a}} = \frac{1}{2} \sqrt{ - \frac{\sum\limits_{i \in \bar{U}} \tau_i a_i^2 - 2f \sum\limits_{i \in \bar{U}} \tau_i a_i + f^2 \sum\limits_{i \in \bar{U}} \tau_i}{\left(d^2 \sum\limits_{i \in \bar{U}} \tau_i + \sum\limits_{i \in U_{\min}} \frac{z_{\min,i}^2}{\tau_i} + \sum\limits_{i \in U_{\max}} \frac{z_{\max,i}^2}{\tau_i} - P_{\mathrm{M}} \right)}} - \hat{\rho}/2. \tag{23}$$

After calculating μ_{a}, λ_{a} can be calculated using (22), and consequently $z_i^* \ \forall i \in \bar{U}$ using (17).

For scenario (ii), having $\mu_{\mathrm{a}} = 0$, λ_{a} can be calculated using (22), then $z_i^* \ \forall i \in \bar{U}$ using (17).

To solve problem $(\mathbf{P3\,a})$, we assume at first that $\alpha_{\mathrm{a},i} = 0 \ \forall i$ and $\nu_{\mathrm{a},i} = 0 \forall i$ i.e. $\bar{U} = \{1, \ldots, K\}$, and assume that $\mu_{\mathrm{a}} = 0$ then we find $z_i^* \ \forall i \in \bar{U}$ and check if they satisfy $\mathbf{C7a}$. If some users violate $\mathbf{C7a}$, the most violated constraint is then satisfied, i.e. its corresponding z_i is set to either $z_{\min,i}$ or $z_{\max,i}$ depending on the violation direction and the previous steps are then repeated again until all users satisfy $\mathbf{C7a}$ then we check if the found solution satisfies the current assumption regarding power budget ($\sum_{i=1}^{K} z_i^2/\tau_i < P_{\mathrm{M}}$) so the algorithm is terminated. Otherwise, we reset the computed users' sets to their default values and restart the algorithm with the assumption that $\mu \neq 0$ as shown in Algorithm I.

C. Fractional Time Allocation

Now, we consider the second subproblem $(\mathbf{P3\,b})$ where $\boldsymbol{\tau}$ vector is optimized while the power allocation vector $\mathbf{z}$ is kept fixed.

$$\begin{aligned} (\mathbf{P3\,b}) \quad \max_{\boldsymbol{\tau}} \quad & -\frac{\hat{\rho}}{2} \sum_{i=1}^{K} \frac{z_i^2}{\tau_i} - \sum_{i=1}^{K} \tilde{g}_i \left(z_i, \tau_i, \bar{z}_i, \bar{\tau}_i \right) \\ \text{subject to} \quad & \mathrm{C1}', \mathrm{C4}, \mathrm{C6}, \\ & \mathrm{C5b} : \tau_i \geq \tau_\epsilon \quad \forall i. \end{aligned}$$

Algorithm I: Weighted current intensity allocation

Input $I, P_{\mathrm{M}}, R_{\mathrm{th}}, \{\gamma_i\}_{i=1}^{K}, \{\tau_i\}_{i=1}^{K}, \{\bar{z}_i\}_{i=1}^{K}, \{\bar{\tau}_i\}_{i=1}^{K}$

Initialize $U_{\min}=\{\}, U_{\max}=\{\}, \bar{U}=\{1,\dots K\}, \mu_{\text{flag}}=0, i=1, O^{+}=0, O^{-}=0$

Compute $\{a_i\}_{i=1}^{K}, \{b_i\}_{i=1}^{K}$ from (6), (7) respectively,$\{\zeta_i\}_{i=1}^{K}$ from (9)

Compute $\{z_{\min,i}\}_{i=1}^{K}, \{z_{\max,i}\}_{i=1}^{K}$ from (10), (11) respectively.

while $i \leq K$ **do**

  if $\mu_{\text{flag}}=0$ **then** $\mu_{\mathrm{a}} \leftarrow 0$

  else Compute from μ_{a} using (23)

  end if

  Compute λ_{a} from (18), then $\{z_i\}_{i\in\bar{U}}$ from (17)

  if $z_{\min,i} < z_i < z_{\max,i} \quad \forall i \in \bar{U}$ **then**

    if $\sum_{i=1}^{K} z_i^2/\tau_i > P_{\mathrm{M}}$ **then**

      $\mu_{\text{flag}} \leftarrow 1$, $U_{\min} \leftarrow \{\}, U_{\max} \leftarrow \{\}, \bar{U} \leftarrow \{1,\dots K\}, O^{+} \leftarrow 0, O^{-} \leftarrow 0$

      Continue

    else

      $\boldsymbol{z}^{*} \leftarrow \boldsymbol{z}, \boldsymbol{\tau}^{*} \leftarrow \boldsymbol{\tau}$

      Terminate the algorithm

    end if

  end if

  Compute $z_i^{\mathrm{uv}} = z_i - z_{\max,i}, z_i^{\mathrm{lv}} = z_{\min,i} - z_i \quad \forall i \in \bar{U}$

  if $\max\limits_{i\in\bar{U}} z_i^{\mathrm{uv}} \geq \max\limits_{i\in\bar{U}} z_i^{\mathrm{lv}}$ and $\max\limits_{i\in\bar{U}} z_i^{\mathrm{uv}} > 0$ **then**

    $\bar{U} \leftarrow \bar{U} - \left\{\arg\max\limits_{i\in\bar{U}} z_i^{\mathrm{uv}}\right\}$, $U_{\max} \leftarrow U_{\max} \cup \left\{\arg\max\limits_{i\in\bar{U}} z_i^{\mathrm{uv}}\right\}$

  else if $\max\limits_{i\in\bar{U}} z_i^{\mathrm{lv}} > \max\limits_{i\in\bar{U}} z_i^{\mathrm{uv}}$ and $\max\limits_{i\in\bar{U}} z_i^{\mathrm{lv}} > 0$ **then**

    $\bar{U} \leftarrow \bar{U} - \left\{\arg\max\limits_{i\in\bar{U}} z_i^{\mathrm{lv}}\right\}$, $U_{\min} \leftarrow U_{\min} \cup \left\{\arg\max\limits_{i\in\bar{U}} z_i^{\mathrm{lv}}\right\}$

  end if

  if $\sum_{i=1}^{K} z_i > I$ and $i = K$ **then**

    $\bar{U} \leftarrow \bar{U} \cup U_{\max}$, $i \leftarrow i - |U_{\max}|$, $U_{\max} = \{\}, O^{+} \leftarrow O^{+} + 1$

  else if $\sum_{i=1}^{K} z_i < I$ and $i = K$ **then**

    $\bar{U} \leftarrow \bar{U} \cup U_{\min}$, $i \leftarrow i - |U_{\min}|$, $U_{\min} = \{\}, O^{-} \leftarrow O^{-} + 1$

  end if

  if $O^{+} > 1$ or $O^{-} > 1$ **then**

    Terminate the algorithm

  end if

end while

It can be shown that C6 and C5b can be reduced to C7b ($\tau_{\min,i} \leq \tau_i \leq \tau_{\max,i} \quad \forall i$), such that:

$$\tau_{\min,i} = \max\left(\tau_\epsilon, \frac{\phi_i - \sqrt{\phi_i^2 - 2\hat{\rho}B_{\rm v}^2 b_i z_i^2}}{2B_{\rm v}b_i}\right), \tag{24}$$

$$\tau_{\max,i} = \frac{\phi_i + \sqrt{\phi_i^2 - 2\hat{\rho}B_{\rm v}^2 b_i z_i^2}}{2B_{\rm v}b_i}, \tag{25}$$

where ϕ_i, is given by:

$$\phi_i = -B_{\rm v}\bar{\tau}_i \ln\left(\frac{e^{-\frac{\bar{z}_i^2}{\bar{\tau}_i^2}\hat{\rho}/2}}{1+\frac{\gamma_i \bar{z}_i^2}{\bar{\tau}_i}}\right) + B_{\rm v}a_i\left(z_i - \bar{z}_i\right) + B_{\rm v}b_i\bar{\tau}_i - \ln(2)R_{\rm th} \tag{26}$$

So $\mathbf{(P3\,b)}$ can be rewritten as:

$$\mathbf{(\tilde{P}3\,b)} \quad \max_{\boldsymbol{\tau}} \qquad -\frac{\hat{\rho}}{2}\sum_{i\in U}\frac{z_i^2}{\tau_i} - \sum_{i\in U}\tilde{g}_i\left(z_i, \tau_i, \bar{z}_i, \bar{\tau}_i\right)$$

$$\text{subject to} \quad \mathrm{C1}', \mathrm{C4}, \mathrm{C7b}.$$

Since this problem is convex and it can be shown that it satisfies Slater's condition then KKT conditions are sufficient for optimality. We solve it by solving its KKT system of equations presented below taking into consideration that strict complementary slackness applies here due to convexity. The Lagrangian function of problem $\mathbf{(\tilde{P}3\,b)}$ can be expressed as:

$$\mathcal{L}_b = -\frac{\hat{\rho}}{2}\sum_{i=1}^{K}\frac{z_i^2}{\tau_i} - \sum_{i=1}^{K}\tilde{g}_i\left(z_i, \tau_i, \bar{z}_i, \bar{\tau}_i\right) + \mu_{\rm b}\left(P_{\rm M} - \sum_{i=1}^{K}\frac{z_i^2}{\tau_i}\right)$$
$$+ \lambda_{\rm b}\left(1 - \sum_{i=1}^{K}\tau_i\right) + \sum_{i=1}^{K}\alpha_{b,i}\left(\tau_i - \tau_{\min,i}\right) + \sum_{i=1}^{K}\nu_{b,i}\left(\tau_{\max,i} - \tau_i\right) \tag{27}$$

The KKT conditions for $\mathbf{(P3\,b)}$ are expressed as:

$$\frac{\partial\mathcal{L}_b}{\partial\tau_i} = \frac{\hat{\rho}}{2}\frac{z_i^2}{\tau_i^2} - b_i + \mu_{\rm b}\frac{z_i^2}{\tau_i^2} - \lambda_{\rm b} + \alpha_{b,i} - \nu_{b,i} = 0 \;\forall i, \tag{28}$$

$\mathrm{C1}', \mathrm{C4}, \mathrm{C7b},$

$$\mu_{\rm b}\left(P_{\rm M} - \sum_{i=1}^{K}\frac{z_i^2}{\tau_i}\right) = 0, \tag{29}$$

$$\lambda_{\rm b}\left(1 - \sum_{i=1}^{K}\tau_i\right) = 0, \tag{30}$$

$$\nu_{b,i}\left(\tau_{\max,i} - \tau_i\right) = 0 \;\forall i, \tag{31}$$

$$\alpha_{b,i}\left(\tau_i - \tau_{\min,i}\right) = 0 \;\forall i. \tag{32}$$

Based on the previous conditions, it can be shown that τ_i^* can be expressed in terms of $\mu_{\rm b}$ and $\lambda_{\rm b}$ as:

$$\tau_i^* = \begin{cases} \tau_{\min,i} \quad \forall i \in U_{\min,\rm b} \\ \sqrt{\left(\frac{\hat{\rho}}{2}+\mu_{\rm b}\right)\frac{z_i^2}{b_i+\lambda_{\rm b}}} \quad \forall i \in \bar{U}_{\rm b} \\ \tau_{\max,i} \quad \forall i \in U_{\max,\rm b} \end{cases}, \tag{33}$$

where $\bar{U}_{\rm b} = \{i : \tau_{\min,i} < \tau_i^* < \tau_{\max,i}\}$, $U_{\min,\rm b} = \{i : \tau_i^* = \tau_{\min,i}\}$, $U_{\max,\rm b} = \{i : \tau_i^* = \tau_{\max,i}\}$, $\bar{U}_b \cup U_{\min,\rm b} \cup U_{\max,\rm b} = \{1,\dots,K\}$, such that $\bar{U}, U_{\min,\rm b},$ and $U_{\max,\rm b}$ are mutually exclusive.

The previous equation implies that $\lambda_{\rm b} \geq -b_{\min}$, where $b_{\min} = \min\limits_i \quad b_i$ and $b_{\max} = \max\limits_i \quad b_i$.

To solve $\mathbf{(P3\,b)}$ we consider two cases: (i) $\mu_{\rm b} = 0$ and (ii) $\mu_{\rm b} \neq 0$.

If $\mu_{\rm b} = 0$, we substitute (33) in C4 to get:

$$\sum_{i=1}^{K} \tau_i = \sqrt{\frac{\hat{\rho}}{2}} \sum_{i\in\bar{U}_{\rm b}} \frac{z_i}{\sqrt{b_i+\lambda_{\rm b}}} + \sum_{i\in U_{\rm b}^{\max}} \tau_{\max,i} + \sum_{i\in U_{\rm b}^{\min}} \tau_{\min,i} = 1 \tag{34}$$

It can be noticed that $\frac{1}{\sqrt{b_{\max}+\lambda_{\rm b}}} \sum\limits_{i\in\bar{U}_{\rm b}} z_i \leq \sum\limits_{i\in\bar{U}_{\rm b}} \frac{z_i}{\sqrt{b_i+\lambda_{\rm b}}} \leq \frac{1}{\sqrt{b_{\min}+\lambda_{\rm b}}} \sum\limits_{i\in\bar{U}_{\rm b}} z_i$. Since the function $\sum\limits_{i\in\bar{U}_{\rm b}} \frac{z_i}{\sqrt{b_i+\lambda_{\rm b}}}$ is a monotonically decreasing function in $\lambda_{\rm b}$ then:

$$\underbrace{\frac{\hat{\rho}\left(\sum\limits_{i\in\bar{U}_{\rm b}} z_i\right)^2}{2\left(1-\sum\limits_{i\in U_{\min}}\tau_{\min,i}-\sum\limits_{i\in U_{\max}}\tau_{\max,i}\right)^2} - b_{\max}}_{\lambda_{\rm b}^{\min}} \leq \lambda_{\rm b} \leq \underbrace{\frac{\hat{\rho}\left(\sum\limits_{i\in\bar{U}_{\rm b}} z_i\right)^2}{2\left(1-\sum\limits_{i\in U_{\min}}\tau_{\min,i}-\sum\limits_{i\in U_{\max}}\tau_{\max,i}\right)^2} - b_{\min}}_{\lambda_{\rm b}^{\max}}.$$

Thus, (34) has exactly one real root for a feasible $U_{\min,\rm b}$ and $U_{\max,\rm b}$ choice. So, it can be solved using bisection method with $\left(\max\left(\lambda_{\rm b}^{\min}, -b_{\min}\right), \lambda_{\rm b}^{\max}\right)$ being the interval of interest. Then, τ_i^* can be calculated easily using (33) with $\mu_{\rm b} = 0$.

In case $\mu_{\rm b} \neq 0$, we have two equality constraints C4 and C1, by substituting (33) in C1 and C4 and after some simple algebraic manipulations, it is proved that:

$$\sum_{(i,j)\in\bar{U}_{\rm b}\times\bar{U}_{\rm b}} \frac{z_i z_j \sqrt{b_j+\lambda_{\rm b}}}{\sqrt{b_i+\lambda_{\rm b}}} = \underbrace{\left(P_{\rm M} - \sum_{i\in U_{\max,\rm b}} \frac{z_i^2}{\tau_{\max,i}} - \sum_{i\in U_{\min,\rm b}} \frac{z_i^2}{\tau_{\min,i}}\right)\left(1 - \sum_{i\in U_{\min,\rm b}} \tau_{\min,i} - \sum_{i\in U_{\max,\rm b}} \tau_{\max,i}\right)}_{\mathcal{R}} \tag{35}$$

$$\sum_{(i,j)\in\bar{U}_{\rm b}\times\bar{U}_{\rm b}} \frac{z_i z_j \sqrt{b_j+\lambda_{\rm b}}}{\sqrt{b_i+\lambda_{\rm b}}} \leq \sum_{i\in\bar{U}_{\rm b}} \frac{z_i}{\sqrt{b_{\min}+\lambda_{\rm b}}} \sum_{j\in\bar{U}_{\rm b}} z_j \sqrt{b_{\max}+\lambda_{\rm b}} = \frac{\sqrt{b_{\max}+\lambda_{\rm b}}}{\sqrt{b_{\min}+\lambda_{\rm b}}} \left(\sum_{i\in\bar{U}_{\rm b}} z_i\right)^2 \tag{36}$$

Also, μ_{b} can be expressed in terms of λ_{b} as:

$$\mu_{\mathrm{b}} = \left(\frac{\sum\limits_{i \in \bar{U}_{\mathrm{b}}} z_i \sqrt{b_i + \lambda_{\mathrm{b}}}}{P_{\mathrm{M}} - \sum\limits_{i \in U_{\max,\mathrm{b}}} \frac{z_i^2}{\tau_{\max,i}} - \sum\limits_{i \in U_{\min,\mathrm{b}}} \frac{z_i^2}{\tau_{\min,i}}} \right)^2 - \frac{\hat{\rho}}{2} \tag{37}$$

The L.H.S of eq. (35) is monotonically decreasing $\forall \lambda_{\mathrm{b}} \geq -b_{\min}$ cf. Appendix C. Also, it is lower bounded by $\sum\limits_{(i,j) \in \bar{U}_{\mathrm{b}} \times \bar{U}_{\mathrm{b}}} z_i z_j$. So (35) can be solved by the bisection method as there is at most one solution for this equation which exists if $\sum\limits_{(i,j) \in \bar{U}_{\mathrm{b}} \times \bar{U}_{\mathrm{b}}} z_i z_j \leq \mathcal{R}$. To get an upper bound for λ_{b}, we upper bound the L.H.S of (35) as follows:

$$\sum_{(i,j) \in \bar{U}_{\mathrm{b}} \times \bar{U}_{\mathrm{b}}} \frac{z_i z_j \sqrt{b_j + \lambda_{\mathrm{b}}}}{\sqrt{b_i + \lambda_{\mathrm{b}}}} \leq \sum_{i \in \bar{U}_{\mathrm{b}}} \frac{z_i}{\sqrt{b_{\min} + \lambda_{\mathrm{b}}}} \sum_{j \in \bar{U}_{\mathrm{b}}} z_j \sqrt{b_{\max} + \lambda_{\mathrm{b}}} = \frac{\sqrt{b_{\max} + \lambda_{\mathrm{b}}}}{\sqrt{b_{\min} + \lambda_{\mathrm{b}}}} \left(\sum_{i \in \bar{U}_{\mathrm{b}}} z_i \right)^2, \tag{38}$$

then we find the intersection between the calculated upper bound of (35) L.H.S and $\mathcal{R}$ to obtain an upper bound on λ_{b} as expressed below:

$$\lambda_{\mathrm{b}} \leq (b_{\max} - b_{\min}) \left(\mathcal{R}^2 / \left(\sum_{i \in \bar{U}_{\mathrm{b}}} z_i \right)^4 - 1 \right)^{-1} - b_{\max} := \bar{\lambda}_{\mathrm{b}}^{\max}. \tag{39}$$

To solve problem $(\mathbf{P3\,b})$, we assume at first that $\alpha_{\mathrm{b},i} = 0 \ \forall i$ and $\nu_{\mathrm{b},i} = 0 \ \forall i$ i.e. $\bar{U} = \{1, \ldots, K\}$, and assume that $\mu_{\mathrm{b}} = 0$ and solve (34) for λ_{b} by bisection method, then we find $\tau_i^* \ \forall i \in \bar{U}$ using (33) and check if they satisfy $\mathbf{C7b}$. If some users violate $\mathbf{C7b}$, the most violated constraint is then satisfied, i.e. its corresponding τ_i is set to either $\tau_{\min,i}$ or $\tau_{\max,i}$ depending on the violation direction and the previous steps are then repeated again until all users satisfy $\mathbf{C7b}$ then we check if the found solution satisfies the current assumption regarding power budget ($\sum_{i=1}^{K} z_i^2/\tau_i < P_{\mathrm{M}}$) so the algorithm is terminated. Otherwise, we reset the computed users' sets to their default values and restart the algorithm with the assumption that $\mu \neq 0$ where we solve (35) for λ_{b}, then we find μ_{b} using (37), and the unknown $\boldsymbol{\tau}$ variables as explained in Algorithm II.

D. Proposed algorithm summary

In this section, we summarize the the resource allocation solution of the VLC downlink cell by introducing the joint power and time allocation (JPTA) algorithm that solves the optimization problem $\mathbf{P1}$ through three nested phases. In the first phase, the equivalent problem $\mathbf{P2}$ is iteratively approximated by different versions of $\mathbf{P3}$ using SCA iterative approach. In the second

Algorithm II: Fractional time allocation

Input $I, P_{\mathrm{M}}, R_{\mathrm{th}}, \{\gamma_i\}_{i=1}^{K}, \{z_i\}_{i=1}^{K}, \{\bar{z}_i\}_{i=1}^{K}, \{\bar{\tau}_i\}_{i=1}^{K}$

Initialize $U_{\min,\mathrm{b}} = \{\}, U_{\max,\mathrm{b}} = \{\}, \bar{U}_{\mathrm{b}} = \{1, \dots K\}, \mu_{\text{flag}} = 0, i = 1$

Compute $\{a_i\}_{i=1}^{K}, \{b_i\}_{i=1}^{K}$ from (6), (7) respectively,$\{\phi_i\}_{i=1}^{K}$ from (26).

Compute $\{\tau_{\min,i}\}_{i=1}^{K}, \{\tau_{\max,i}\}_{i=1}^{K}$ from (24), (25) respectively.

while $i \leq K$ **do**

  if $\mu_{\text{flag}} = 0$ **then Solve** (34) for λ_{b}, $\mu_{\mathrm{b}} \leftarrow 0$

  else Solve (35) for λ_{b}, then **Compute** μ_{b} from (37)

  end if

  Compute $\{\tau_i\}_{i \in \bar{U}_{\mathrm{b}}}$ from (33)

  if $\tau_{\min,i} < \tau_i < \tau_{\max,i} \quad \forall i \in \bar{U}_{\mathrm{b}}$ **then**

    if $\sum_{i=1}^{K} z_i^2/\tau_i > P_{\mathrm{M}}$ **then**

      $\mu_{\text{flag}} \leftarrow 1$, $U_{\min,\mathrm{b}} \leftarrow \{\}, U_{\max,\mathrm{b}} \leftarrow \{\}, \bar{U}_{\mathrm{b}} \leftarrow \{1, \dots K\}, O^{+} \leftarrow 0, O^{-} \leftarrow 0$

      Continue

    else

      $\boldsymbol{\tau}^{*} \leftarrow \boldsymbol{\tau}$

      Terminate the algorithm

    end if

  end if

  Compute $\tau_i^{\mathrm{uv}} = \tau_i - \tau_{\max,i}, \tau_i^{\mathrm{lv}} = \tau_{\min,i} - \tau_i \quad \forall i \in \bar{U}_{\mathrm{b}}$

  if $\max_{i \in \bar{U}_{\mathrm{b}}} \tau_i^{\mathrm{uv}} \geq \max_{i \in \bar{U}_{\mathrm{b}}} \tau_i^{\mathrm{lv}}$ and $\max_{i \in \bar{U}_{\mathrm{b}}} \tau_i^{\mathrm{uv}} > 0$ **then**

    $\bar{U}_{\mathrm{b}} \leftarrow \bar{U}_{\mathrm{b}} - \left\{ \arg\max_{i \in \bar{U}_{\mathrm{b}}} \tau_i^{\mathrm{uv}} \right\}$, $U_{\max,\mathrm{b}} \leftarrow U_{\max,\mathrm{b}} \cup \left\{ \arg\max_{i \in \bar{U}_{\mathrm{b}}} \tau_i^{\mathrm{uv}} \right\}$

  else if $\max_{i \in \bar{U}_{\mathrm{b}}} \tau_i^{\mathrm{lv}} > \max_{i \in \bar{U}_{\mathrm{b}}} \tau_i^{\mathrm{uv}}$ and $\max_{i \in \bar{U}_{\mathrm{b}}} \tau_i^{\mathrm{lv}} > 0$ **then**

    $\bar{U}_{\mathrm{b}} \leftarrow \bar{U}_{\mathrm{b}} - \left\{ \arg\max_{i \in \bar{U}_{\mathrm{b}}} \tau_i^{\mathrm{lv}} \right\}$, $U_{\min,\mathrm{b}} \leftarrow U_{\min,\mathrm{b}} \cup \left\{ \arg\max_{i \in \bar{U}_{\mathrm{b}}} \tau_i^{\mathrm{lv}} \right\}$

  end if

  if $\sum_{i=1}^{K} \tau_i > 1$ and $i = K$ **then**

    $\bar{U}_{\mathrm{b}} \leftarrow \bar{U}_{\mathrm{b}} \cup U_{\max,\mathrm{b}}$, $i \leftarrow i - |U_{\max,\mathrm{b}}|$, $U_{\max,\mathrm{b}} = \{\}$, $O^{+} \leftarrow O^{+} + 1$

  else if $\sum_{i=1}^{K} \tau_i < 1$ and $i = K$ **then**

    $\bar{U}_{\mathrm{b}} \leftarrow \bar{U}_{\mathrm{b}} \cup U_{\min,\mathrm{b}}$, $i \leftarrow i - |U_{\min,\mathrm{b}}|$, $U_{\min,\mathrm{b}} = \{\}$, $O^{-} \leftarrow O^{-} + 1$

  end if

  if $O^{+} > 1$ or $O^{-} > 1$ **then**

    Terminate the algorithm

  end if

end while

Algorithm III: Joint power and time allocation (JPTA)

Input $I, P_{\mathrm{M}}, R_{\mathrm{th}}, \{\gamma_i\}_{i=1}^{K}$
Find a feasible initial point $\boldsymbol{z}^{\mathrm{init}}$ and $\boldsymbol{\tau}^{\mathrm{init}}$ using Algorithm IV.
Initialize $\boldsymbol{z} \leftarrow \boldsymbol{z}^{\mathrm{init}}, \boldsymbol{\tau} \leftarrow \boldsymbol{\tau}^{\mathrm{init}}, \boldsymbol{z}^{*} \leftarrow \boldsymbol{z}^{\mathrm{init}}, \boldsymbol{\tau}^{*} \leftarrow \boldsymbol{\tau}^{\mathrm{init}}$
while $\Delta_{\mathrm{outer}} > \epsilon_{\mathrm{outer}}$ **do**
    while $\Delta_{\mathrm{inner}} > \epsilon_{\mathrm{inner}}$ **do**
        Solve $(\mathbf{P3\,a})$ to update $\boldsymbol{z}^{*}$ using Algorithm I.
        Solve $(\mathbf{P3\,b})$ to update $\boldsymbol{\tau}^{*}$ using Algorithm II.
        Compute Δ_{inner} as the difference between the latest two objective function values of $(\mathbf{P3})$
    end while
    Compute Δ_{outer} as the difference between the latest two objective function values of $(\tilde{\mathbf{P}}\mathbf{1})$
end while
Output $\boldsymbol{z}^{*}$ and $\boldsymbol{\tau}^{*}$ and compute $\boldsymbol{x}^{*}$.

phase, each formulated version of $\mathbf{P3}$ is solved iteratively by solving $\mathbf{P3a}$ and $\mathbf{P3b}$ in an alternating manner till the stopping criterion is met. The last inner phase of the JPTA algorithm solves $\mathbf{P3a}$ and $\mathbf{P3b}$ based on KKT conditions using Algorithm I and Algorithm II respectively, where different configurations for the dual variables associated with inequality constraints are scanned based on the complementary slackness possibilities till a configuration is found that satisfies stationarity conditions and primal feasibility.

IV. Problem feasibility and starting point calculation

Due to the complexity of the feasibility region considered in this paper, it is not easy to determine the problem feasibility nor to get an initial point $\left(\boldsymbol{\tau}^{\mathrm{init}}, \mathbf{z}^{\mathrm{init}}\right)$ to start the SCA process. To this end we formulate $(\mathbf{P0})$, if this problem is feasible, and its minimum objective value is less than P_{M}, then $(\tilde{\mathbf{P}}\mathbf{1})$ is feasible and the solution of $(\mathbf{P0})$ can be used as an initial point for the SCA iterations.

Algorithm IV: Initial Point Calculation

Input $I, P_{\mathrm{M}}, R_{\mathrm{th}}, \{\gamma_i\}_{i=1}^{K}$
Solve $(\bar{\mathbf{P}}_{\mathbf{V}}\mathbf{0})$ to get $I_{\min}$ the minimum illumination for feasibility
if $I_{\min} > I$ **then**
    Terminate (The problem is considered infeasible).
else
    Solve $(\tilde{\mathbf{P}}_{\mathbf{V}}\mathbf{0})$ to get $P_{\min}$ and $\boldsymbol{z}^{\mathrm{init}}, \boldsymbol{\tau}^{\mathrm{init}}$
    if $P_{\min} > P_{\mathrm{M}}$ **then**
        Terminate (The problem is considered infeasible).
    end if
end if
Output $\boldsymbol{z}^{\mathrm{init}}, \boldsymbol{\tau}^{\mathrm{init}}$.

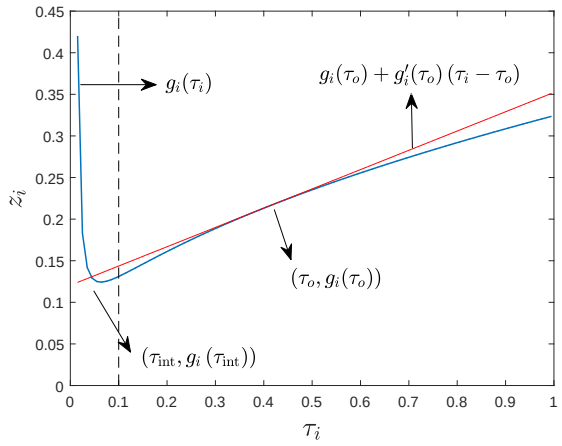

Fig. 4: Rate constraint feasibility space

$$(\mathbf{P0}) \quad \min_{\mathbf{z},\boldsymbol{\tau}} \quad \sum_{i=1}^{K} \frac{z_i^2}{\tau_i}$$
$$\text{subject to} \quad \mathrm{C2}', \mathrm{C3}', \mathrm{C4}-\mathrm{C5}$$

It can be noticed that the constraints of $(\mathbf{P0})$ represent a convex set except for $\mathrm{C3}'$ which is not convex for all values of z_i and τ_i. However, a necessary condition on the convexity of the set represented by the simultaneity of $\mathrm{C3}'$ and $\mathrm{C5}$ can be obtained as follows:

C6 along with $z_i \geq 0 \ \forall i$ is equivalent to $z_i \geq g_i(\tau_i) \ \forall i$, where $g_i(\tau_i) = \frac{\tau_i}{\sqrt{\gamma_i}} \sqrt{\left(e^{\frac{2R_{\text{th}} \ln(2)}{\tau_i B_{\text{v}}}} - 1 \right)}$.

Based on the previous discussion, $\mathbf{(P0)}$ is equivalent to:

$$\begin{aligned} \min_{\mathbf{z},\boldsymbol{\tau}} \quad & \sum_{i=1}^{K} \frac{z_i^2}{\tau_i} \\ \text{subject to} \quad & \text{C2}', \text{C4}, \text{C5}, \\ & \text{C8} : z_i \geq g_i(\tau_i) \quad \forall i. \end{aligned}$$

The feasibility region is convex if $\frac{d^2 g_i}{d\tau_i^2} \geq 0$ which is expressed as

$$\frac{\left(\frac{2R_{\text{th}}}{B_{\text{v}}}\right)^2 \ln^2(2) 2^{\frac{2R_{\text{th}}}{\tau_i B_{\text{v}}} - 2} \left(2^{\frac{2R_{\text{th}}}{\tau_i B_{\text{v}}}} - 2 \right)}{\sqrt{\gamma_i} \tau_i^3 \left(2^{\frac{2R_{\text{th}}}{\tau_i B_{\text{v}}}} - 1 \right)^{3/2}} \geq 0. \tag{40}$$

Thus, one can easily show that the convexity condition is equivalent to $R_{\text{th}} \geq \frac{\tau_i B_{\text{v}}}{2} \ \forall i$. In addition, since $\tau_i \leq 1$, $R_{\text{th}} \geq \frac{B_{\text{v}}}{2}$ becomes a sufficient condition for the convexity of $g_i(\tau_i)$ and the problem as well. On the other hand, if the convexity condition is not satisfied, we use the following approximated convex problem

$$\begin{aligned} \mathbf{(\tilde{P}0)} \quad \min_{\mathbf{z},\boldsymbol{\tau}} \quad & \sum_{i=1}^{K} \frac{z_i^2}{\tau_i} \\ \text{subject to} \quad & \text{C2}', \text{C4}, \text{C5}, \text{C8}, \\ & \text{C9} : z_i \geq g_i(\tau_o) + g_i'(\tau_{o,i})(\tau_i - \tau_{o,i}) \quad \forall i, \end{aligned}$$

where we add C9 to the constraints set to ensure the convexity of the feasibility region which can be seen in Fig. 4 as the area above the curve and the tangent line drawn that represents (C9 :) needs to be chosen carefully to have a good convex approximation for the original feasibility region. It is worthy mentioning that $\tau_{o,i}$ should be greater than τ', such that $\tau' = 2R_{\text{th}}/B_{\text{v}}$ (inflection point of $g_i(\tau_i) \ \forall i$) and less than 1. We choose $\tau_{o,i}$ that minimizes the discarded area from the original feasibility region defined by rate constraint due to approximation (the area between the blue curve and the tangent line as shown in Fig. 4) that is expressed as follows:

$$\mathcal{A}(\tau_{o,i}) = \int_{\tau_{\text{int}}(\tau_{o,i})}^{1} \left(g_i(\tau_{o,i}) + g_i'(\tau_{o,i})(\tau_i - \tau_{o,i}) - g_i(\tau_i) \right) d\tau_i, \tag{41}$$

where $g_i\left(\tau_{o,i}\right)+g_i'\left(\tau_{o,i}\right)\left(\tau_{\text{int}}\left(\tau_{o,i}\right)-\tau_{o,i}\right)=g_i\left(\tau_{\text{int}}\left(\tau_{o,i}\right)\right)$, which can be rewritten as:

$$\frac{\tau_{o,i}}{\sqrt{\gamma_i}}\sqrt{\left(e^{\frac{2R_{\text{th}}\ln(2)}{\tau_{o,i}B_{\text{v}}}}-1\right)}+\frac{B_{\text{v}}\tau_{o,i}\left(e^{\frac{2R_{\text{th}}\ln(2)}{\tau_{o,i}B_{\text{v}}}}-1\right)-2R_{\text{th}}\ln(2)e^{\frac{2R_{\text{th}}\ln(2)}{\tau_{o,i}B_{\text{v}}}}}{\sqrt{\gamma_i}B_{\text{v}}\tau_{o,i}\sqrt{\left(e^{\frac{2R_{\text{th}}\ln(2)}{\tau_{o,i}B_{\text{v}}}}-1\right)}}\left(\tau_{\text{int}}-\tau_{o,i}\right)$$

$$=\frac{\tau_{\text{int}}}{\sqrt{\gamma_i}}\sqrt{\left(e^{\frac{2R_{\text{th}}\ln(2)}{\tau_{\text{int}}B_{\text{v}}}}-1\right)}. \tag{42}$$

By multiplying the previous equation by $\sqrt{\gamma_i}$, it becomes clear that τ_{int} does not vary for each user because of channel variations. Similarly it can be proved that the optimal $\tau_{o,i}$ is constant for all users, i.e. $\tau_{o,i}^*=\tau_o^*$. This fact implies that the scheduler can calculate τ_o^* for the required QoS given the available bandwidth once, and use it as long as these factors are kept constant. We find τ_o^* by exhaustive search over the range $[\tau',1]$.

In order to investigate the feasibility of $(\tilde{\mathbf{P}}\mathbf{0})$, we need to solve the following problem and check that the optimal value is less than I.

$$(\bar{\mathbf{P}}\mathbf{0}) \quad \min_{\mathbf{z},\boldsymbol{\tau}} \quad \sum_{i=1}^{K} z_i$$
$$\text{subject to} \quad \text{C4}, \text{C5}, \text{C8}, \text{C9},$$

which is a convex optimization problem that we solve with interior point method.

So, to check the feasibility of $(\tilde{\mathbf{P}}\mathbf{1})$, we first solve $(\bar{\mathbf{P}}\mathbf{0})$ to make sure that $(\tilde{\mathbf{P}}\mathbf{0})$ is feasible, otherwise we consider that $(\tilde{\mathbf{P}}\mathbf{1})$ is infeasible. Then, we solve $(\tilde{\mathbf{P}}\mathbf{0})$ and check, if the optimal objective obtained is less than P_{M} then $(\tilde{\mathbf{P}}\mathbf{1})$ is feasible and the obtained solution is $\boldsymbol{\tau}^{\text{init}}, \mathbf{z}^{\text{init}}$ to start the SCA otherwise, $(\tilde{\mathbf{P}}\mathbf{1})$ is considered infeasible.

V. Computational Complexity analysis

In this section, we analyze the computation complexity of the proposed JPTA algorithm. The complexity is analyzed in terms of the number of evaluations needed for all variables, which is written as

$$C_{\tilde{\mathbf{P}}\mathbf{1}}=I_{\text{SCA}}I_{\text{Alt}}(C_{\mathbf{P3a}}(K)+C_{\mathbf{P3b}}(K)), \tag{43}$$

where $C_{\mathbf{P3a}}(K)$ and $C_{\mathbf{P3b}}(K)$ represent the number of computation evaluations for both $\boldsymbol{z}$ and $\boldsymbol{\tau}$, respectively, I_{SCA} is the number of SCA iterations and I_{Alt} is the number of alternate optimization iterations.

TABLE I: Default Simulation Parameters.

$N_0 = 10^{-21}$ W/Hz	$B_{\rm v} = 20$ MHz	$H = 4.5$ m	$\phi_{\rm A} = 40^\circ$	$h_{\rm T} = 0.85$ m
$P_{\rm M} = 28$ W	$K = 5$	$R_{\rm th} = 50000$ bps	$\tau_\epsilon = 10^{-8}$ s	$I = 2.1$ A
$A_{\rm PD} = 1\,{\rm cm}^2$	$\eta_{\rm oe} = R_{\rm PD} = 0.6$A/W	$R = 6.32$ m	$\eta_{\rm eo} = 1$	

Firstly, we evaluate $C_{\mathbf{P3a}}(K)$ based on Algorithm I assuming worst case, where it needs takes $2K$ iterations to calculate the sets $\bar{U}$, $U_{\max}$, and $U_{\min}$ or terminate. In each iteration when $\mu_{\rm a} = 0$, $\lambda_{\rm a}$ is calculated in addition to a number of $\boldsymbol{z}$ variables that decreases linearly by one in each iteration, which results in $2\sum_{i=1}^{K}(i+1) = K^2 + 3K$ variable computations. On the other hand, when $\mu_{\rm a} \neq 0$ the calculations will include $\mu_{\rm a}$ computation giving $2\sum_{1}^{K}(i+2) = K^2 + 5K$ unkonwn variable computations. As a result, we have $C_{\mathbf{P3a}}(K) = 2K^2 + 8K$.

Secondly, we find $C_{\mathbf{P3b}}(K)$ from Algorithm II, which is very similar to $C_{\mathbf{P3a}}(K)$, except that $\lambda_{\rm b}$ does not have closed form expression as $\lambda_{\rm a}$. In Algorithm II, $\lambda_{\rm b}$ is calculated using bisection method with $\log_2\left(\frac{\lambda_{\rm b}^{\max} - \max\left(\lambda_{\rm b}^{\min}, -b_{\min}\right)}{\epsilon_\lambda}\right)$ and $\log_2\left(\frac{\lambda_{\rm b}^{\max} + b_{\min}}{\epsilon_\lambda}\right)$ iterations for $\mu_{\rm b} = 0$ and $\mu_{\rm b} \neq 0$, respectively, where ϵ_λ is the tolerable error in $\lambda_{\rm b}$. Hence, the overall complexity reduces to $2\sum_{i=1}^{K}\left(i + \log_2\left(\frac{\lambda_{\rm b}^{\max} - \max\left(\lambda_{\rm b}^{\min}, -b_{\min}\right)}{\epsilon_\lambda}\right)\right)$ for $\mu_{\rm b} = 0$, and $2\sum_{i=1}^{K}\left(i + 1 + \log_2\left(\frac{\bar{\lambda}_{\rm b}^{\max} + b_{\min}}{\epsilon_\lambda}\right)\right)$ for $\mu_{\rm b} \neq 0$. Consequently, $C_{\mathbf{P3b}}(K)$ is expressed as

$$C_{\mathbf{P3b}}(K) = 2K^2 + 4K + 2K\left(\log_2\left(\frac{\lambda_{\rm b}^{\max} - \max\left(\lambda_{\rm b}^{\min}, -b_{\min}\right)}{\epsilon_\lambda}\right) + \log_2\left(\frac{\bar{\lambda}_{\rm b}^{\max} + b_{\min}}{\epsilon_\lambda}\right)\right). \tag{44}$$

It is worth to discuss also the compuation complexity of the feasibility problems used before executinh the JPTA algorithm. Since both $(\tilde{\mathbf{P}}\mathbf{0})$ and $(\bar{\mathbf{P}}\mathbf{0})$ are solved using the interior point method algorithm, the number of variable computations can be given, respectively, as [24]:

$$C_{\tilde{\mathbf{P}}\mathbf{0}} = \alpha_1 \max\left((2K)^3, (2K)^2(4K+2), \left(2K + 4K^2\right)(4K+3)\right), \tag{45}$$

and

$$C_{\bar{\mathbf{P}}\mathbf{0}} = \alpha_2 \max\left((2K)^3, (2K)^2(4K+1), \left(2K + 4K^2\right)(4K+2)\right), \tag{46}$$

where α_1 and α_2 are the number of iterations.

VI. Simulation results

The simulation setup consists of a large indoor area as in a lecture hall or a library section where a single VLC transmitter at the ceiling at a height H from the ground. The receivers clearance from ground surface is assumed to be h_{T}. We assume that receivers are uniformly distributed over a circle of radius R m centered around the transmitter which is horizontally oriented as the receivers as shown in Fig. 3. The average SE presented results are calculated based on 1000 realizations of users placed at random locations according to uniform distribution on the coverage circle surface. Unless otherwise stated, we use the simulation parameters listed in Table I. We assume line-of-sight existence for all links.

In this section, we study the performance of four different solutions for the considered SE maximization problem, namely, the JPTA, an upper bound for it where we do SCA but solve $(\mathbf{P3})$ optimally using interior point method (JPTA int.), the initial solution found by Algorithm II which aims at power minimization subject to the same original constraints, and the uniform allocation scheme, where power and time budgets are divided equally between users i.e. minimum rate violation could occur (SE of this realization is set to zero). In the following simulations realizations that are considered infeasible are assumed to have zero SE when the average SE is calculated.

In the first simulation, we study the effect of increasing number of users on the SE performance of the three algorithms as shown in Fig. 5. The unimodal behavior seen vs K owes back to two facts; the first is that for small K values as K increases the transmitter gets better chances of having users with better channel gains (higher degrees of freedom) without having much pressure from the rate requirement constraints with the available power budget. The second fact is that when K gets large enough, feasibility space becomes tightly squeezed by rate constraints that force losses in SE performance. That is because the transmitter becomes obligated to allocate more resources to users experiencing bad channels, and even worse infeasible problem instances which contribute with zero SE to the monitored average SE metric, become more frequent.

In the second simulation, as can be noticed in Fig. 6 that for small values of I, the system experiences outage because rate requirements can not be satisfied as I is less than minimum I value required for feasibility (optimal value of problem $\bar{\mathrm{P}}0$). Moreover, the system will experience outage for large values of I, where available power budget is insufficient to satisfy the illumination and rate requirements. The SE performance is improved when I increases because

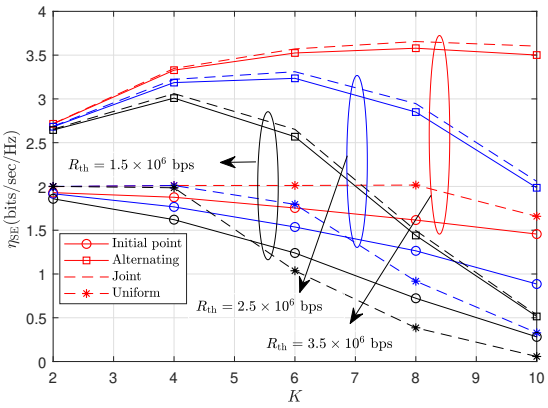

Fig. 5: Average SE vs Number of Users

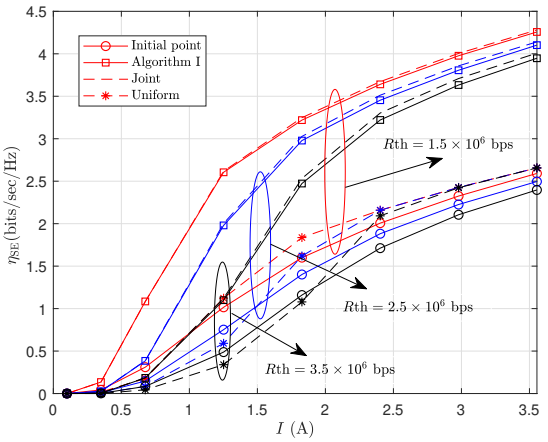

Fig. 6: Average SE vs Illumination Current Intensity

the feasibility region becomes larger which implies that probability of problem feasibility gets larger. In addition, performance gaps between SCA based algorithms (JPTA and JPTA interior point) and the initial solution (power minimization) are enlarged, because of the conflicting objectives of the algorithms, which is highlighted as the degrees of freedom available for the system increases by increasing I. In the third simulation, we study the effect of increasing radius of the circle where users are distributed uniformly on the SE performance of the system. It can be seen in Fig. 7 that as users are distributed over larger circles, the attainable SE gets worsened because as this happens users are more likely to have worse channel gains as they get further. However, optimization gains gets larger, i.e. gaps between initial point solution SE performance and both interior point based approach, and the alternating optimization approach get wider.

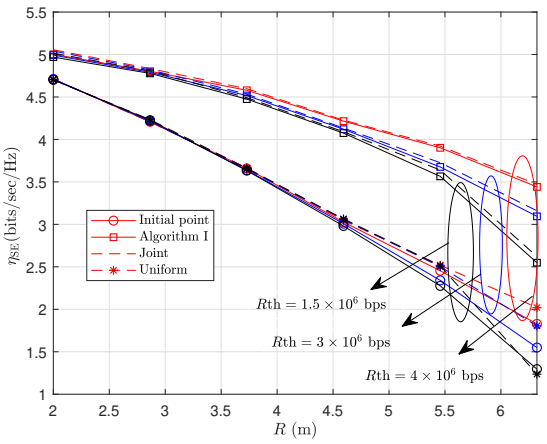

Fig. 7: Average SE vs Radius of distribution

In the fourth simulation, the effect of increasing the transmitter half-power beamwidth on the SE of the system is studied for the three allocation strategies, which is depicted in Fig. 8. It is observed that as ϕ_{A} increases, the SE experiences a unimodal behavior, because for a very small beamwidth, only users near the transmitter will experience good channels, while users near the cell edge will suffer. In other words, as beamwidth increases, far users start to get better channels and near users lose partially their channel gain, this loss is outweighed by the improvement of far users channel gains from the SE performance perspective till the beamwidth reaches a critical value, above which SE performance deteriorates as channel gains of far users either stop to get enhanced (because the transmitter power is being distributed over a larger area than that occupied by the users), or that gain becomes less than the loss of channel gains for near users. Moreover, it can be seen that for low values of ϕ_{A} the slope of the curve is sharper than for large values, because of large number of infeasible cases when transmitter beamwidth is narrow. However, for large ϕ_{A} values channels deterioration, which degrades the SE performance in consequence, is not as severe. That is because, it does not encompass a lot of infeasible instances of the problem. It can be noticed as well that as R_{th} increases the optimal beamwidth increases, due to increase of infeasible cases chances for low ϕ_{A} values.

It can be noticed in all simulations that, as R_{th} increases, the performance gaps between the proposed SCA approaches and using the initial point solution decreases, as the feasibility space becomes smaller, and the available resources become hardly sufficient to cover the increased rate requirements. Moreover, number of infeasible problems is increased which have the same zero

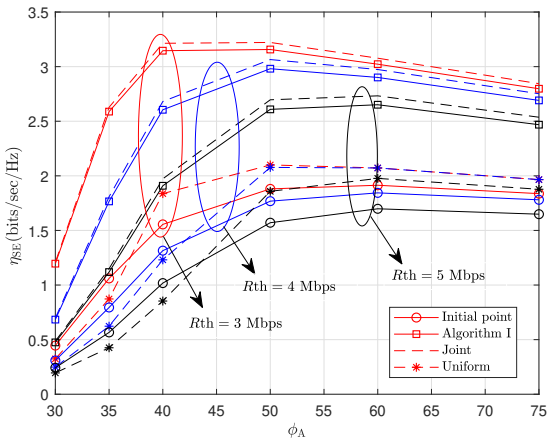

Fig. 8: Average SE vs Transmitter Half Power Beamwidth

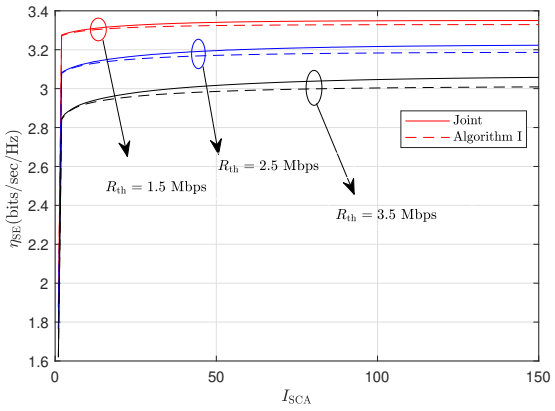

Fig. 9: Average SE vs number of iterations

SE performance contribution, hence the average performances of the considered algorithms get closer. A similar observation can be noticed for the uniform allocation solution as well. It can be seen also that in all simulations as the problem constraints become tighter, the uniform allocation approach solution gets outperformed by the initial point solution, although initial point solution always attempts to achieve a conflicting objective with SE (minimizing energy consumption), this owes to the increase of number of infeasible realizations for uniform allocation as constraints get tighter.

In Fig. 9, we plot the average SE performance achieved by using the JPTA algorithm and the JPTA interior point algorithm for different values of R_{th} as the number of iterations of the loop responsible for the SCA procedure increases. In this simulation, the value of the

objective function is kept fixed when convergence is reached. The presented simulation results shows consistent average monotonically increasing behavior for the objective functions which demonstrates the effectiveness and the convergence rate of the proposed algorithm.

VII. Conclusion

In this work, we proposed an algorithm with low-complexity to solve the non-convex joint time and power allocation problem for a VLC system employing dynamic TDMA having illumination, power budget, and minimum rate constraints. To solve this problem, we first showed that it can be modeled as DC programming problem then we solved each of the convex problems encountered in each iteration of SCA by alternating optimization, where the optimization problems found therein are solved based on a KKT approach. We proposed a method to detect feasibility of this hard problem. We compared our proposed algorithm with the obtained initial solution of the feasibility problem and with another approach, where we solve the SCA problems using interior point method, and the simulation results showed that the performance gap between the formerly mentioned approach and ours is small, whilst both of them significantly outperform the initial point solution. The proposed resource allocation algorithm provieds a therotical lower bound performance limit that can be conisidered a good benchmark for future practical adaptive VLC modulation schemes.

Appendix A

In this appendix we prove proposition 1. It can be noticed that $f(\tau, z; \gamma) = \tau \ln\left(1 + \gamma \frac{z^2}{\tau^2}\right)$ is the perspective transform[2] of $\ln(1 + \gamma z^2)$. Since the perspective transform preserves convexity/concavity, we decompose $\ln(1 + \gamma z^2)$ into a difference of two concave functions format, then take the perspective transform of that decomposition to obtain DC decomposition for $f(\tau, z; \gamma)$. For this purpose, we express $\ln(1 + \gamma z^2)$ as

$$\log\left(1 + \gamma z^2\right) = h(z) - g(z), \tag{47}$$

where $h(z)$ and $g(z)$ are defined, respectively, as

$$h(z) = \ln\left(f\left(z\right)\right), \tag{48}$$

$$g(z) = \ln\left(\frac{f\left(z\right)}{\left(1 + \gamma z^2\right)}\right). \tag{49}$$

[2]The perspective transform of $f(z)$ with respect to t is $tf(\frac{z}{t})$ $t > 0$ and it maintains the function convexity/concavity.

To ensure that $h(z)$ and $g(z)$ are concave, we need to find $f(z)$ such that $h''(z) = \frac{d^2h(z)}{dz^2} \leq 0$ and $g''(z) = \frac{d^2g(z)}{dz^2} \leq 0$. First, we express $h''(z)$ and $g''(z)$, respectively, as

$$h''(z) = \frac{f(z)f''(z) - \left(f'(z)\right)^2}{f^2(z)}, \tag{50}$$

$$g''(z) = \frac{f(z)f''(z) - \left(f'(z)\right)^2}{f^2(z)} - 2\gamma\frac{1-\gamma z^2}{\left(1+\gamma z^2\right)^2}, \tag{51}$$

where $f'(z) = \frac{df(z)}{dz}$ and $f''(z) = \frac{d^2f(z)}{dz^2}$. Then, we express (51) in terms of (50) as

$$g''(z) = h''(z) - 2\gamma\frac{1-\gamma z^2}{\left(1+\gamma z^2\right)^2} \tag{52}$$

Define $U = h''(z) + \rho$, where

$$\rho = \max_{z} \quad -2\gamma\frac{1-\gamma z^2}{\left(1+\gamma z^2\right)^2} = \frac{\gamma}{4}. \tag{53}$$

Therefore, if $U \leq 0$, then $g''(z) \leq 0$ which guarantees that $h''(z) \leq 0$ since ρ is positive. As such, the concavity conditions for both $h(z)$ and $g(z)$ are satisfied if $U \leq 0$ that can be achieved by solving the following differential equation

$$f(z)f''(z) - \left(f'(z)\right)^2 + \rho f^2(z) = 0. \tag{54}$$

One can find that the solution of (54) is obtained in the following general form (cf. Appendix B for proof)

$$f(z) = c_2 e^{zc_1 - z^2\rho/2}. \tag{55}$$

A possible choice is obtained by setting $c_2 = 1$ and $c_1 = 0$ as

$$f(z) = e^{-z^2\rho/2}. \tag{56}$$

To this end, we have proved that, $\ln\left(1+\gamma z^2\right)$ can be decomposed into a difference of two concave functions as:

$$\ln\left(1+\gamma z^2\right) = -\frac{\rho z^2}{2} - \ln\left(\frac{1+\gamma z^2}{e^{-\frac{\rho z^2}{2}}}\right). \tag{57}$$

By taking the perspective transform of the previous equation, we get:

$$\tau\ln\left(1+\gamma\frac{z^2}{\tau^2}\right) = -\frac{\rho z^2}{2\tau} - \tau\ln\left(\frac{1+\gamma\frac{z^2}{\tau^2}}{e^{-\frac{\rho z^2}{2\tau^2}}}\right), \tag{58}$$

which concludes the proof.

APPENDIX B

In this section we prove that the solution of (54) is given by (55).

$$f''(z) - \frac{(f'(z))^2}{f(z)} + \rho f(z) = 0 \tag{59}$$

Let $W(z) = (f'(z))^2$. By using this substitution, we can reformulate (54) to be:

$$w'(f) - \frac{2}{f} w + 2\rho f = 0 \tag{60}$$

This is a linear first order differential equation that can be solved as follows:

$$w(f) = \frac{1}{u(f)} \int u(f) q(f) df, \quad u(f) = e^{\int -\frac{2}{f} df},\ q(f) = -2\rho f \tag{61}$$

Therefore,

$$w(f) = f^2 \left(a - 2\rho \ln(f)\right), \tag{62}$$

where a is constant. Now to obtain $f(z)$, we need to solve the following equation:

$$(f'(z))^2 = f(z)^2 \left(a - 2\rho \ln(f(z))\right) \tag{63}$$

By separating variables and integrating both sides we get,

$$\int \frac{df}{f\sqrt{a - 2\rho \ln(f)}} = \int dz \tag{64}$$

$$-\frac{\sqrt{a - 2\rho \ln(f)}}{\rho} = z + b, \text{where } b \text{ is a constant} \tag{65}$$

$$a/\rho^2 - 2\ln(f)/\rho = (z+b)^2 \tag{66}$$

$$f(z) = e^{\left(-\rho z^2/2 - \rho z b - \rho\left(b^2 - a/\rho^2\right)/2\right)} \tag{67}$$

$$f(z) = c_2 e^{\left(\rho z c_1 - \rho z^2/2\right)} \tag{68}$$

APPENDIX C

In this section we prove the monotonicity of the L.H.S of (35).

$$\text{L.H.S} = \sum_{(i,j)\in \bar{U}_\text{b}\times\bar{U}_\text{b}} \frac{z_i z_j \sqrt{b_j + \lambda_\text{b}}}{\sqrt{b_i + \lambda_\text{b}}} = \sum_{\substack{(i,j)\in \bar{U}_\text{b}\times\bar{U}_\text{b}, \\ i<j}} z_i z_j \left(\frac{\sqrt{b_j + \lambda_\text{b}}}{\sqrt{b_i + \lambda_\text{b}}} + \frac{\sqrt{b_i + \lambda_\text{b}}}{\sqrt{b_j + \lambda_\text{b}}}\right) + \sum_{i\in\bar{U}_\text{b}} z_i^2 \tag{69}$$

$$= \sum_{\substack{(i,j)\in \bar{U}_\text{b}\times\bar{U}_\text{b}, \\ i<j}} z_i z_j \frac{b_i + b_j + 2\lambda_\text{b}}{\sqrt{b_i + \lambda_\text{b}}\sqrt{b_j + \lambda_\text{b}}} + \sum_{i\in\bar{U}_\text{b}} z_i^2 \tag{70}$$

For the L.H.S to be real, $(b_i + \lambda_{\rm b})\,(b_j + \lambda_{\rm b}) \geq 0 \ \forall (i,j) \in \bar{U}_{\rm b} \times \bar{U}_{\rm b}$, which implies that $\lambda_{\rm b} \geq -b_i \ \forall i \in \bar{U}_{\rm b}$ or $\lambda_{\rm b} \leq -b_i \ \forall i \in \bar{U}_{\rm b}$. However, we are interested in the former condition to keep $\tau_i^* \ \forall i \in \bar{U}_{\rm b}$ real.

By calculating the first derivative of L.H.S with respect to $\lambda_{\rm b}$, we get:

$$\frac{\partial}{\partial \lambda_{\rm b}} \text{L.H.S} = \sum_{\substack{(i,j)\in \bar{U}_{\rm b}\times \bar{U}_{\rm b}, \\ i<j}} -z_i z_j \frac{(b_i - b_j)^2}{\sqrt{b_i + \lambda_{\rm b}}^3 \sqrt{b_j + \lambda_{\rm b}}^3} \leq 0, \ \lambda_{\rm b} \geq -b_i \ \ \forall i \in \bar{U}_{\rm b} \tag{71}$$

REFERENCES

[1] A. M. Abdelhady, O. Amin, A. Chaaban, and M. S. Alouini, "Downlink resource allocation for multichannel TDMA visible light communications," in *2016 IEEE Global Conference on Signal and Information Processing (GlobalSIP)*, Dec 2016, pp. 1–5.

[2] M. A. Khalighi and M. Uysal, "Survey on free space optical communication: A communication theory perspective," *IEEE Commun. Surveys Tuts.*, vol. 16, no. 4, pp. 2231–2258, Jun. 2014.

[3] C.-X. Wang, F. Haider, X. Gao, X.-H. You, Y. Yang, D. Yuan, H. Aggoune, H. Haas, S. Fletcher, and E. Hepsaydir, "Cellular architecture and key technologies for 5G wireless communication networks," *IEEE Commun. Mag.*, vol. 52, no. 2, pp. 122–130, Feb. 2014.

[4] D. Zheng, G. Chen, and J. A. Farrell, "Joint measurement and trajectory recovery in visible light communication," *IEEE Trans. Control Syst. Technol.*, vol. 25, no. 1, pp. 247–261, Jan 2017.

[5] P. H. Pathak, X. Feng, P. Hu, and P. Mohapatra, "Visible light communication, networking, and sensing: A survey, potential and challenges," *IEEE Communications Surveys Tutorials*, vol. 17, no. 4, pp. 2047–2077, Fourthquarter 2015.

[6] J. Gancarz, H. Elgala, and T. D. C. Little, "Impact of lighting requirements on VLC systems," *IEEE Communications Magazine*, vol. 51, no. 12, pp. 34–41, December 2013.

[7] A. M. Abdelhady, O. Amin, A. Chaaban, and M. S. Alouini, "Resource allocation for outdoor visible light communications with energy harvesting capabilities," in *2017 IEEE Globecom Workshops (GC Wkshps)*, Dec 2017, pp. 1–6.

[8] A. Chaaban, Z. Rezki, and M.-S. Alouini, "Capacity bounds for parallel IM-DD optical wireless channels," in *Accepted in International Conference on Communications (ICC)*, Kuala Lumpur, 2016.

[9] C. Gong, S. Li, Q. Gao, and Z. Xu, "Power and rate optimization for visible light communication system with lighting constraints," *IEEE Trans. Signal Process.*, vol. 63, no. 16, pp. 4245–4256, Aug. 2015.

[10] R. Jiang, Z. Wang, Q. Wang, and L. Dai, "Multi-user sum-rate optimization for visible light communications with lighting constraints," *J. Lightw. Technol.*, vol. 34, no. 16, pp. 3943–3952, Aug 2016.

[11] W. Y. Wang, Y. J. Zhu, Y. Y. Zhang, and J. K. Zhang, "An optimal power allocation for multi-LED phase-shifted-based MISO VLC systems," *IEEE Photon. Technol. Lett.*, vol. 27, no. 22, pp. 2391–2394, Nov 2015.

[12] H. Shen, Y. Deng, W. Xu, and C. Zhao, "Rate maximization for downlink multiuser visible light communications," *IEEE Access*, vol. 4, pp. 6567–6573, Sep. 2016.

[13] ——, "Rate-maximized zero-forcing beamforming for VLC multiuser MISO downlinks," *IEEE Photon. Technol. Lett.*, vol. 8, no. 1, pp. 1–13, Feb 2016.

[14] D. Bykhovsky and S. Arnon, "Multiple access resource allocation in visible light communication systems," *J. Lightw. Technol.*, vol. 32, no. 8, pp. 1594–1600, Apr. 2014.

[15] S. Shao, A. Khreishah, and I. Khalil, "Joint link scheduling and brightness control for greening VLC-based indoor access networks," *IEEE/OSA Journal of Optical Communications and Networking*, vol. 8, no. 3, pp. 148–161, March 2016.

[16] F. Jin, X. Li, R. Zhang, C. Dong, and L. Hanzo, "Resource allocation under delay-guarantee constraints for visible-light communication," *IEEE Access*, vol. 4, pp. 7301–7312, May 2016.

[17] H. Elgala, R. Mesleh, and H. Haas, "Indoor optical wireless communication: potential and state-of-the-art," *IEEE Communications Magazine*, vol. 49, no. 9, pp. 56–62, September 2011.

[18] H. Haas and S. McLaughlin, "A dynamic channel assignment algorithm for a hybrid tdma/cdma-tdd," *IEEE J. Sel. Areas Commun.*

[19] G. V. Tsoulos, "Smart antennas for mobile communication systems: benefits and challenges," *Electron. Commun. Eng. J.*, vol. 11, no. 2, pp. 84–94, April 1999.

[20] S. Dimitrov and H. Haas, *Principles of LED light communications: towards networked Li-Fi*. Cambridge University Press, 2015.

[21] T. Jiang, L. Song, and Y. Zhang, *Orthogonal frequency division multiple access fundamentals and applications*. CRC Press, 2010.

[22] J. M. Kahn and J. R. Barry, "Wireless infrared communications," *Proceedings of the IEEE*, vol. 85, no. 2, pp. 265–298, Feb 1997.

[23] A. Lapidoth, S. M. Moser, and M. Wigger, "On the capacity of free-space optical intensity channels," *IEEE Trans. Inf. Theory*, vol. 55, no. 10, pp. 4449–4461, Oct. 2009.

[24] S. Boyd and L. Vandenberghe, *Convex optimization*. Cambridge university press, 2004.